

MIT Open Access Articles

*Ultrafast, low-power, PCB manufacturable,
continuous-flow microdevice for DNA amplification*

The MIT Faculty has made this article openly available. **Please share**
how this access benefits you. Your story matters.

Citation: Kaprou, Georgia D. et al. "Ultrafast, low-power, PCB manufacturable, continuous-flow microdevice for DNA amplification." *Analytical and Bioanalytical Chemistry* 411 (June 2019): 5297-307 ©2019 Author(s)

As Published: 10.1007/s00216-019-01911-1

Publisher: Springer Berlin Heidelberg

Persistent URL: <https://hdl.handle.net/1721.1/128675>

Version: Author's final manuscript: final author's manuscript post peer review, without publisher's formatting or copy editing

Terms of Use: Article is made available in accordance with the publisher's policy and may be subject to US copyright law. Please refer to the publisher's site for terms of use.



Ultrafast, low-power, PCB manufacturable, continuous-flow microdevice for DNA amplification

Cite this article as: Georgia D. Kaprou, Vasileios Papadopoulos, Dimitris P. Papageorgiou, Ioanna Kefala, George Papadakis, Electra Gizeli, Stavros Chatzandroulis, George Kokkoris, Angeliki Tserepi, Ultrafast, low-power, PCB manufacturable, continuous-flow microdevice for DNA amplification, *Analytical and Bioanalytical Chemistry*, doi: [10.1007/s00216-019-01911-1](https://doi.org/10.1007/s00216-019-01911-1)

This Author Accepted Manuscript is a PDF file of a an unedited peer-reviewed manuscript that has been accepted for publication but has not been copyedited or corrected. The official version of record that is published in the journal is kept up to date and so may therefore differ from this version.

Terms of use and reuse: academic research for non-commercial purposes, see here for full terms.

<http://www.springer.com/gb/open-access/authors-rights/aam-terms-v1>

Author accepted manuscript

Ultrafast, low-power, PCB manufacturable, continuous-flow microdevice for DNA amplification

Georgia D. Kaprou^{a,b}, Vasileios Papadopoulos^a, Dimitris P. Papageorgiou^{a,#}, Ioanna Kefala^a, George Papadakis^c, Electra Gizeli^{b,c}, Stavros Chatzandroulis^a, George Kokkoris^{a,*}, Angeliki Tserepi^{a,*}

^a Institute of Nanoscience and Nanotechnology, NCSR Demokritos, Patr. Gregoriou E' and 27 Neapoleos Str., PO Box 60037, 15341 Agia Paraskevi, Attica, Greece

^b Department of Biology, Univ. of Crete, Voutes, 70013 Heraklion, Greece

^c Institute of Molecular Biology and Biotechnology-FORTH, 100 N. Plastira Str., 70013 Heraklion, Greece

[#] Current address: Department of Materials Science and Engineering, Massachusetts Institute of Technology, Cambridge, MA 02139, USA

*Corresponding authors, e-mail:

George Kokkoris: g.kokkoris@inn.demokritos.gr

Angeliki Tserepi: a.tserepi@inn.demokritos.gr

Abstract

The design and fabrication of a continuous flow μ PCR device with very short amplification time and low power consumption is presented. Commercially available, 4-layer printed circuit board (PCB) substrates are employed, with in-house designed yet industrially manufactured embedded Cu micro-resistive heaters lying at very close distance from the microfluidic network, where DNA amplification takes place. The 1.9 m-long microchannel in combination with desirably high flow velocities (for fast amplification) challenged the robustness of the sealing, that was overcome with the development of a novel bonding method rendering the microdevice robust even at extreme pressure drops (12 bars). The proposed fabrication methods are PCB compatible, allowing for mass and reliable production of the μ PCR device in the established PCB industry. The μ PCR chip was successfully validated during the amplification of two different DNA fragments (and with different target DNA copies) corresponding to the exon 20 of the BRCA1 gene, and to the plasmid pBR322, a commonly used cloning vector in *E. coli*. Successful DNA amplification was demonstrated at total reaction

times down to 2 min, with a power consumption of 2.7 W, rendering the presented μ PCR one of the fastest and lowest power consuming devices, suitable for implementation in low-resource settings. Detailed numerical calculations of the DNA residence time distributions, within an acceptable temperature range for denaturation, annealing and extension, performed for the first time in the literature, provide useful information regarding the actual on-chip PCR protocol and justify the maximum volumetric flow rate for successful DNA amplification. The calculations indicate that the shortest amplification time is achieved when the device is operated at its enzyme kinetic limit (i.e., extension rate).

Keywords MicroPCR; continuous-flow; PCB substrates, computational fluid dynamics; heat transport; residence time distribution;

1. Introduction

During the last two decades, miniaturization processes possess a crucial role for innovations in life sciences, analytical sciences, diagnostics and bio/chemistry, and have led to the development of the so-called micro total analysis systems (μ TAS) or lab-on-a-chip (LOC) [1-3]. The implementation of such devices enables the development of fast, easy-to-use and portable systems with a high level of automation and functional integration for applications such as point-of-care (POC) diagnostics for health [4], point-of-need (PON) systems for environmental monitoring [5] and food analysis [6-9], forensics [10], and drug development [11].

Polymerase chain reaction (PCR) is the most established nucleic acid amplification method, developed by Kary Mullis in 1983 [12]. PCR mimics the natural DNA replication process. It is a temperature mediated enzyme catalyzed reaction allowing for exponential amplification of very small amounts of DNA or RNA rendering it an extremely powerful tool for reliable and rapid nucleic acid detection. Many analytical microdevices performing the PCR (micro-PCR or μ PCR devices) have been extensively reported due to the gravity of this processing step in various bio-analytical assays [13-16].

The majority of μ PCR devices [4, 17] can be categorized in two well-defined types: static chamber (SC) μ PCR devices [18, 19] –mimicking in their operation the conventional thermocycler– and continuous flow (CF) [20-23] μ PCR devices. In static chamber μ PCR devices, the injected mixture along with the whole chip undergoes thermal cycling following a specific temperature protocol. Consequently, SC μ PCR devices are usually characterized by larger thermal inertia compared to the CF devices, leading to longer PCR duration and higher energy consumption. In fact, a significant reduction in the PCR duration (from hours to minutes) was observed due to the shift from external heaters to

integrated ones [4, 24] (due to significant reduction in thermal mass). Total amplification times ranging from 5 to 30 min have been reported in static chamber μ PCR devices integrated with microheaters. On the contrary, in CF μ PCR devices only the injected PCR mixture undergoes thermal cycling (smaller thermal inertia), as it flows across the distinct heated zones corresponding to the (2 or 3) temperature steps needed for PCR. In addition, thermal equilibration between the substrate and the sample is faster in CF than in SC μ PCR devices, due to their higher surface to volume ratio. Thus, in CF μ PCR devices, rapid nucleic acid amplification has been achieved (between 90 s and 15 min) and thus the energy requirement is reduced [25], allowing for more energy-efficient devices amenable to portable POC/PON systems.

Despite the roaring interest in POC diagnostics, stemming from their development in recent years, very few POC devices have reached the market [26, 27]. The main challenge for successful commercialization of microfluidic devices is scaling-up, i.e. the translation of prototype miniaturized devices into industrial mass production [9, 28, 29], where fabrication technologies play a crucial role.

During the last decade, there is a growing interest in employing printed circuit boards (PCB) as (rigid or flexible) substrates for developing microfluidic devices [30-33]. The industrial availability of the well-established PCB technology for the mass production of consumer electronics and electronic circuits, in combination with the low cost of the substrates, renders it tremendously appealing. Furthermore, the integration possibilities for sensors, actuators, electronics and microfluidics offered by the employment of PCBs are remarkable.

Numerous implementations of PCB technology to microfluidic applications have been presented up to now in the literature [33]. Very early work on fabrication of PCB-based microfluidics suggested the use of copper (Cu) as a structural material for the microfluidic network [30, 34]. However, Cu is not biocompatible due to its known cytotoxicity [35] and inhibition of biological processes (e.g. DNA amplification) [36]. Therefore, different materials such as polymeric ones were sought as structural materials and respective processes were developed for PCB-based microfluidic devices implemented in (bio)chemical analysis.

Fabrication of microfluidic networks has been presented on polyimide films, photosensitive (e.g. PI2732, DuPont) or non-photosensitive ones (e.g. PI2611, Pyralux™, from DuPont) [22, 37, 38]. In many cases, a broadly used epoxy resist, namely SU-8, has been employed as a structural material to form microfluidic structures on PCB [32, 39]. In addition, dry film photoresists (DFR) such as 1002F (also known as TMMF) and TMMR S2000 (also known as TMMF S2000) have been employed for encapsulation, planarization, formation and sealing of microfluidic structures on PCB [39-41].

To promote and ease the mass production of microfluidic devices, the research community has proposed materials with which the PCB industry is particularly familiar. One example is double-sided tapes enclosed by PCBs [42] to form

microfluidic structures where electrochemical sensors were incorporated for on-chip detection of biomarkers. Our team has pioneered polyimide-based laminated DFRs recently implemented for the formation of microfluidics such as micromixers [43, 44] and an isothermal DNA amplification microdevice [45] on commercial PCBs.

In microfluidics fabrication, sealing processes are also of high importance, and indeed sealing is weighed by experts as one of the crucial practical challenges [46, 47] and a main hindrance for microfluidics commercialization, in addition to standardization and integration [26]. The microfluidics community lacks suitable materials for sealing massively, easily, inexpensively; robustly and irreversibly devices where high pressure drops are anticipated.

Herein a CF μ PCR device is designed, fabricated and validated for the amplification of different in length and number of copies DNA fragments: 157 bp DNA fragments corresponding to the exon 20 of the BRCA1 gene, as well as 198 bp and 395 bp DNA fragments of the plasmid pBR322 (at 20-fold lower target DNA copies), a commonly used cloning vector in *E. coli*. For the device sealing, we propose the introduction of suitable materials, already established and employed in the PCB industry, nevertheless for a completely different purpose, i.e. for the robust sealing of microfluidic devices where both high temperatures (nearly 100 °C) are required and high pressures drops (in long microchannels) are developed during their operation. These materials are routinely implemented in the PCB industry as standard for electrical insulation and environmental protection of the Cu structures on PCBs, but it is the first time that they are implemented for the sealing of extremely long microchannels that are demonstrated robust for pressure drops up to 12 bars. The introduction of these materials, in combination with the previously described [45, 48] formation of embedded resistive microheaters within the PCB substrate, renders the herein described integrated microfluidic device for DNA amplification perfectly suitable and easy to manufacture in large scale and low cost by PCB manufacturers, thus facilitating the commercialization of such DNA-based bioanalytical microdevices. Therefore, the μ PCR device introduced herein combines many advantages: it is one of the fastest CF devices reported in the literature (amplification at the enzyme kinetic limit), operating well at high flow rates (15 μ l/min) thanks to the robustness of the sealing process, completely manufacturable in the established PCB industry thus paving the way to complete fabrication of such μ PCR devices in a widespread industry, and at the same time of low power consumption. Therefore, the presented device combines unique advantages never met before in a *single device*.

Besides the realization and the validation of the μ PCR device, the actual PCR protocol held on the device is investigated through a computational study. The actual PCR protocol, differs from the nominal one (obtained from the ratios of the volume of each zone over the volumetric flow rate) due to the velocity and the temperature distribution of the sample within the μ PCR device. The aim is to explain the results of the validation of the device and investigate the potential for further improvement of the design. The actual PCR protocol can be estimated by the calculation of the residence time of DNA molecules in a short or acceptable range around the temperatures of denaturation, annealing, and extension. The

protocol is calculated as a function of the volumetric flow rate and is used to justify the dependence of DNA amplification (obtained from standard agarose gel electrophoresis) on the implemented flow rates.

The residence time in each one of the three temperature ranges is calculated by the combination of a detailed 3D modeling framework [22, 25] for the calculation of the velocity and the temperature field with a Lagrangian model for the calculation of molecule trajectories. It is pointed out that the use of Lagrangian models is rare in the literature of μ PCR devices [49] and that the residence time distributions of the DNA molecules within the acceptable temperature ranges (for denaturation, annealing and extension) are calculated for the first time in a CF μ PCR device.

2. Materials and methods

2.1. Chip design

The μ PCR device comprising both a microfluidic network and embedded resistive microheaters implements by design 30 thermal cycles in total for the efficient amplification of DNA. Since each PCR cycle comprises three thermal steps in the implemented protocol, three discrete thermal zones are designed. Each thermal zone is defined by an individual resistive microheater lying at a small distance beneath a part of the meandering microfluidic channel (Fig. S1, see Electronic Supplementary Material, ESM). The total length of the meandering microchannel is 1.9 m. As the PCR sample flows continuously across the three PCR temperature zones, it is thermocycled.

The embedded resistive microheaters were designed for realization in the inner Cu layer (thickness of 18 μ m) of the commercially available PCB substrate. The total thickness of the PCB substrate is 1.5 mm. The microheaters were designed using Kicad, an open source software suitable for electronic design automation (EDA), to exhibit an electrical resistance of approximately 44, 37 and 58 Ohm, for the denaturation, annealing and extension zone, respectively. The designs were sent to a PCB manufacturer (Eurocircuits N.V., Belgium) for the realization of devices in large numbers.

2.2 Fabrication Process

A 4-Cu layer PCB [with a 710 μ m flame-retardant (FR4) core] is used for the fabrication (at the PCB industry) of the resistive microheaters, which extend over two (inner) Cu layers [50]. For the formation of the microchannel on the PCB substrates with already embedded microheaters, a commercially available, PCB compatible photoimageable dry film, the Pyralux® PC1015 was used. The Pyralux® PC1000 materials (from Dupont™) are flexible photoimageable coverlays and solder masks used at the PCB industry to encapsulate flexible printed circuitry. Composed of a specially developed

combination of acrylic, urethane, and imide-based material, they are negative-tone, aqueous processable resists, offering a patterning resolution of $< 100 \mu\text{m}$. They exhibit robust chemical resistance and can withstand high temperatures and humidity. They are thus suitable as structural materials of microreactors performing biological reactions that require high temperatures, such as PCR (denaturation step performed at $95 \text{ }^\circ\text{C}$), and are implemented as such in this work, according to the method described in detail in ESM. Fig. S1b (see ESM) depicts the process flow for the seamless fabrication of the DNA amplification microdevice on commercially available PCB substrates.

After patterning of the microchannel on the PCB with embedded Cu microheaters, manufactured at the PCB industry, sealing of the microchannel followed with the DuPont™ Pyralux® LF coverlay, a thermally assisted pressure sensitive sealing film. It consists of DuPont Kapton® polyimide film, coated on one side with a proprietary B-staged modified acrylic adhesive. The total thickness of the coverlay is $152 \mu\text{m}$ ($25 \mu\text{m}$ and $127 \mu\text{m}$ for the adhesive and the Kapton backing, respectively). The long length of the microfluidic channel, in combination with the high flow rates and temperatures ($95 \text{ }^\circ\text{C}$) employed during operation, renders the sealing process of the μPCR device extremely demanding. However, the process developed (patent application [51], [52]) offers a simple method for irreversible and robust sealing for microfluidic devices even with high pressure drops during operation. The compatibility of the materials used as well as of the implemented patterning and sealing processes with the established PCB industry allows for the manufacturing of the described μPCR at the PCB industry, at a low cost. The total volume of the fabricated μPCR devices is $30 \mu\text{l}$, comparable to typical bench-top reaction volumes. Fig. 1 shows a) a PCB substrate with three embedded microheaters and b) a fabricated continuous flow μPCR device before its sealing. The 30 PCR cycles are accommodated by the 30 meanders of the 1.9 m long microchannel and the three microheaters (corresponding to denaturation, annealing and extension) viewed beneath the microchannel as dark zones in the PCB.

2.3 Microheater characterization and temperature control

For the characterization of the resistive microheaters, a probe station was employed with a heated base (Signatone S-1041-D3 Hot chuck) and a Keithley 2400 source-meter controlled by Labview, for sourcing current I and measuring electrical resistance R . The heaters were vacuum attached onto a hot plate of controlled temperature. The electrical resistance for various temperatures within the range of interest ($25\text{-}100 \text{ }^\circ\text{C}$) were recorded and the temperature coefficient of resistance (TCR), associating the microheater resistance to their temperature, was determined;

$$R = R_0 + R_0 \times \text{TCR} \times (T - T_0) \quad (1)$$

where R is the microheater resistance at temperature T , R_0 is the microheater resistance at reference temperature (i.e. 20 °C), T is the microheater temperature, and T_0 is the reference temperature at which the microheater resistance is measured.

The microheaters have a dual role; they are used as heating elements as well as temperature sensors to provide feedback for temperature control of the μ PCR thermal zones. To adjust the temperatures appropriate for the PCR protocol to be performed, a custom-made temperature control unit was developed. It was built based on a microcontroller capable of controlling and reading the onboard Digital to Analog and Analog to Digital Converters (DACs and ADCs) and communicate with a personal computer. The temperature controller is capable of controlling independently up to three resistive microheaters corresponding to the three different thermal zones necessary for a PCR protocol. Temperature control is obtained by controlling the voltage across each resistive microheater, while a small sensing resistor is used to measure the current flowing through them.

2.4 PCR sample preparation and evaluation of amplification

For the evaluation of the amplification efficiency of the fabricated μ PCR devices, a 250 bp fragment from the exon 20 of the BRCA1 gene was used. For its amplification, a set of primers (Forward: 5'- TCC TGA TGG GTT GTG TTT GG-3' and Reverse: 5'-TGG TGG GGT GAG ATT TTT GTC-3') [53] were employed which produce a 157 bp amplicon. In addition, the plasmid pBR322 with a size of 4361 bp, which is a commonly used cloning vector in *E. coli* containing the genes for resistance to ampicillin and tetracycline, was used as a DNA template. For its amplification, two sets of primers [(Forward: 5' - CCA CCA AAC GTT TCG GCG AG-3' and Reverse 198: 5'-GCT GTC CC T GAT GGT CGT CA -3') and (Forward: 5' - CCA CCA AAC GTT TCG GCG AG-3' and Reverse 395 5'-GCCGGCTTCCATTCAGGTCG -3')] were employed producing a 198 bp and a 395 bp amplicon, respectively.

PCR amplification was performed according to the manufacturer's instructions (KAPA Biosystems, KAPA 2G Fast Hot Start readymix) [54]. 5 pmoles of each primer were mixed for short human DNA fragment with KAPA 2G Fast DNA polymerase (KAPA Biosystems) according to the manufacturer protocol. Each PCR reaction was supplemented with $MgCl_2$ and Bovine Serum Albumin (BSA) to a final concentration of 2.5 mM and 100 μ g/ml, respectively. BSA was added as blocking agent, to prevent adsorption of biological sample on microchannel walls during the actual μ PCR experiments. 1 μ l of DNA template with a concentration of 0.5 ng/ μ l was used per 30 μ l of reaction. 0.5 ng of the DNA template correspond to 2×10^9 copies for the short human DNA template and 10^8 copies for the plasmid DNA template, thus the efficiency of the μ PCR device was evaluated at two different DNA target copies. For on-chip PCR, first, the temperature of the resistive

microheaters was set to 95 °C, 55 °C and 72 °C for the denaturation, annealing and extension step, respectively. After temperature equilibration of the microheaters (evidenced through their resistance measurement), 30 µl of reaction mix were introduced in the µPCR device, flowing through the microchannel at 6 different volumetric flow rates: 2.5, 5, 7.5, 10, 15 and 20 µl/min. The amplification protocol used in the conventional thermocycler consisted of 1 min initial denaturation at 95 °C, 30 cycles of 10 s denaturation at 95 °C – 10 s annealing at 55 °C – 10 s extension at 72 °C and a final 1 min extension at 72 °C. PCR products were loaded on a 2% agarose gel stained with ethidium bromide (more information in Section S3 of the ESM) and visualized with an ultraviolet (UV) transilluminator.

Semi-quantified results can be obtained from the agarose gel images, analyzed by means of imageJ software. The intensity of each amplicon band obtained at different flow rates was normalized to the ladder's band intensity corresponding to 200 bp, and finally relative intensities were obtained with respect to the band intensity at 2.5 µl/min.

2.5 Numerical calculations

Critical for the efficiency of the DNA amplification is the residence time of DNA molecules in each one of the three temperatures of the PCR. A simple rule to implement a PCR protocol in a continuous flow µPCR device is to combine the volume of each thermal zone with the volumetric flow rate so as to achieve the desired protocol. The ratio of the volume of a zone over the volumetric flow rate is an estimation of the time duration that the PCR mixture remains in the thermal zone. However, given that the velocity profile is not uniform inside the microchannel and that the temperature uniformity is not ideal within each thermal zone, the calculation of the residence time of the DNA molecules in a small temperature range around the set points of PCR is not straightforward. For this reason, the velocity profile as well as the temperature distribution inside the microchannel are required. If we consider that a DNA molecule remains on the same streamline during its “journey” in the microchannel (massless particles with neutral buoyancy), the temperature that the molecule “feels” is the temperature along this streamline. A video demonstrating the temperature that a molecule “feels” is provided as a video in ESM. The time interval that the DNA molecule remains in a temperature range is the residence time of the molecule in this range. The residence times of a large number of DNA molecules in the denaturation (or annealing or extension) range traveling along different streamlines compose the residence time distribution (RTD) for the denaturation (or annealing or extension) range. The residence time of DNA molecules in a temperature range is the mean value of the pertinent RTD.

The velocity profile and the temperature distribution inside the microchannel is calculated by a detailed 3D modeling framework [25] consisting of the heat transfer equation in the solid layers of the device and the fluid (PCR mixture), the momentum conservation and continuity equations, and the current density conservation equation, the latter describing the Joule heating phenomenon in the heaters. The modeling framework is complemented with the equations for the calculation of the streamlines. All calculations are performed in a unit cell of the device (Fig. 2), i.e. in the part of the device where one thermal cycle takes place. Details of the procedure followed are included in Section S4 of the ESM.

3. Results and Discussion

3.1 Experimental results

i. Characterization of microheaters and their power consumption

Fig. 1a shows a PCB substrate with three embedded Cu microheaters fabricated in a major PCB manufacturer following the specifications set by our CAD file. For the characterization of these microheaters, their electrical resistance for various temperatures within the range 25-100 °C were recorded. These measurements were repeated for various resistive microheaters in order to determine an average value of the TCR which is an inherent property of the material (i.e., Cu). An average TCR of $0.0036 \text{ }^{\circ}\text{C}^{-1} \pm 0.0002 \text{ }^{\circ}\text{C}^{-1}$ was estimated which is in agreement (within less than 10%) with values reported in the literature [55, 56]. A representative resistance versus temperature curve for a microheater can be found in Section S2 of the ESM (Fig. S3).

As the temperature values achieved on the resistive microheaters are essential for successful and highly efficient PCR reactions, the temperature was independently measured directly on the sealing layer of the device, which is the material in closest contact with the heated DNA sample. Thus, the temperature of each of the three thermal zones above each resistive microheater was measured independently using an external platinum (Pt) thermometer. The temperatures measured with the Pt thermometer were in excellent agreement with the temperatures set on the resistive microheaters by means of the temperature controller (through the measured TCR value).

The characterization of the PCB microheaters was followed by the evaluation of their power consumption for achieving the desirable temperatures for denaturation (95 °C), annealing (55 °C), and extension (72 °C). This involved the use of the custom-made temperature controller unit which records the current, the voltage, and the resulting power consumption for each resistive microheater. For a μ PCR device with a set of PCB microheaters (with resistances R_{01} , R_{02} and R_{03} equal to

44.2 Ohm, 57.2 Ohm and 37 Ohm respectively, R_0 measured at 25°C), the current, the voltage and thus the power consumption were recorded during device operation. Table 1 illustrates the power consumption measured for each heater after temperature stabilization at the indicated set points.

Table 1 Power requirements of the microheaters for achieving PCR-relevant temperatures

Zone	R_0 (Ohm)	T_0 (°C)	T (°C)	Power (W)
denaturation	44.2	25	95	1.627
extension	57.2	25	72	0.792
annealing	37	25	55	0.246

Therefore, the total power consumption during operation of the μ PCR device is 2.7 W, comparable to the power consumption of energy efficient μ PCR devices [24, 57]. The measured total power consumption is in good agreement with the calculated one (2.3W) through numerical calculations (data not shown) with a deviation less than 15%. This very low power consumption combined with the short total reaction time (as will be shown below) renders it a very efficient μ PCR device with respect to energy requirements. It is estimated that with regular lithium batteries (2000mAh) found in power banks for laptops (14.8V cell voltage) more than 300 PCR reactions can run with the present μ PCR (1 reaction consumes 324 J). Up to date, only very few continuous-flow, fast and at the same time low power consuming (up to a few W) μ PCR devices have been presented in the literature [Wheeler et al (444 J) [58], Moschou et al (690 J) [22], Jiang et al. (48 J) [59]] including the present one (324 J), which position themselves at the forefront for implementation in POC systems in resource limited settings.

ii. Robustness of sealing

Before using the μ PCR devices for biological experiments, sealed devices were tested in terms of robustness of their sealing. With the aid of a custom made chip holder (enabling the fluidic interface), the μ PCR device was connected to a syringe pump and it was tested for flow rates ranging from 1-100 μ l/min, at room temperature, without observing any delamination of the sealing layer and subsequent leakage. The pressure drop across the microchannel at the flow rate of 100 μ l/min is 12.4 bars, demonstrating that the sealed microdevices were capable of withstanding pressures higher than 12 bars at room temperature. The same tests were performed at elevated temperatures. In more detail, the heaters were set at 95 °C,

55 °C and 72 °C for the denaturation, annealing and extension zones, respectively, and flow rates up to 100 $\mu\text{l}/\text{min}$ were used, without any delamination of the sealing layer.

iii. Evaluation of the amplification efficiency

Once the temperature equilibration of the microheaters was achieved, 30 μl of reaction mix were introduced in the μPCR device. Fig. 3 shows two agarose gel electrophoresis images depicting bands of DNA amplicons obtained at different flow rates, i.e. 5, 7.5 and 10 $\mu\text{l}/\text{min}$ (gel images for the rest of the flow rates through the μPCR are provided in Figs. S3a and S3b of the ESM). For comparison, each gel image contains also the DNA ladder (on the left of all images). By comparing the bands of amplified products and the DNA ladder, we verified amplification of the correct DNA product at 157 bp, at flow rates as high as 15 $\mu\text{l}/\text{min}$ (2 min total reaction time, shown in ESM Figs. S3a and S3b), while no amplification was observed at 20 $\mu\text{l}/\text{min}$. Although the amplified product is 157 bp, the gel images (of the product on the cyclor and the μPCR) depict the amplicons closer to the 200 bp ladder band. This can be attributed to the higher viscosity of the samples loaded on the gels (containing BSA for microchannel wall passivation), since no DNA purification step was carried out after the DNA amplification. The results support successful DNA amplification in the fabricated devices flowing through the microchannel at 5 different volumetric flow rates: 2.5, 5, 7.5, 10, and 15 $\mu\text{l}/\text{min}$. The total amplification time for 30 PCR cycles was 12, 6, 4, 3 and 2 min, respectively. These amplification times correspond to approximately 21.6, 10.8, 7.2, 5.4 and 3.6 s per PCR cycle. Conventional benchtop thermocyclers are impossible to achieve such fast cycles, due to limitations in the temperature ramping rates. Typically, more than 30 min are required to perform a 30 cycle PCR reaction depending on the thermocycler's specifications. Indeed, when the same temperature protocol described above was used to perform a PCR reaction in a conventional thermocycler (iCycler™, BIO-RAD), with a residence time of 10 s in each zone/temperature (as recommended for the commercial kit), a 30 cycle PCR was completed in 45 min. The amplicon band intensity obtained with the thermocycler was 4.5% more intense than with the μPCR at a volumetric flow rate of 2.5 $\mu\text{l}/\text{min}$. Therefore, the DNA amplification efficiency of the μPCR (at 2.5 $\mu\text{l}/\text{min}$) is very comparable to that of the thermocycler, at a total reaction time reduced by a factor of 3.75. The PCR reaction can be performed in the present microdevice even 22 times faster (at 15 $\mu\text{l}/\text{min}$, data shown in ESM Fig. S3a), nevertheless at the expense of amplification efficiency. Semi-quantified results obtained from the agarose gel images are presented in Table 2 and indicate a reduction of the band intensity with the increase of the volumetric flow rate, due to reduction of the nominal residence time of the PCR cocktail in each thermal zone. Despite the intensity reduction by almost an order of magnitude (to 19%) at the very high flow rates (15 $\mu\text{l}/\text{min}$), we demonstrate amplification of the DNA (signal above the noise level) at an impressive PCR duration of 2 min.

This constitutes the continuous flow μ PCR device reported herein one of the fastest ones reported so far in the literature (90 s [20]).

The μ PCR was also validated during the amplification of much longer (4361 bp) DNA templates, and of 20-fold lower target DNA copies. Fig. 4 shows two agarose gel electrophoresis images depicting bands of DNA amplicons with a size of 198 bp (a) and 395 bp (b) stemming from the amplification of the plasmid DNA obtained at a flow rate of 7.5 μ l/min. The images indicate very efficient amplification for the 198 bp amplicon, and weaker amplification for the 395 bp amplicon, as expected by the longer (by a factor of 2) extension time required. Despite the fact that the validation with plasmid DNA was performed only at a single flow rate (7.5 μ l/min), the high fluorescence signal of the amplicon band indicates that amplification would be possible at even higher flow rates (or amplification times less than 3.6 min). In all cases, the results demonstrate the applicability of this CF μ PCR device in the efficient amplification of various DNA templates, different products and target DNA copies, at a reaction time at least one order of magnitude smaller than that of a conventional cyclor. The target copies of plasmid DNA (10^8) for which efficient amplification was obtained in the present μ PCR device are comparable to those in similar devices; the same as in Kopp et al. (10^8) [20], comparable to or little higher than those in Hashimoto et al. (2×10^7 - 2×10^8) [60], and lower than those in Moschou et al. (7×10^8 - 7×10^9) [22]. Therefore, the present device exhibits comparable sensitivity to reported equally fast μ PCR devices. Of paramount importance is the fact that this μ PCR is industrially manufacturable at low cost and thus can facilitate the way for standardization and commercialization of microfluidic devices implemented in molecular POC diagnostics.

Table 2 Total PCR time, one-cycle duration, and relative band intensity versus the volumetric flow rate through the μ PCR device

Volumetric flow rate (μ l/min)	Total reaction time (min)	Cycle duration (s)	Band intensity (%)
2.5	12	21.6	100
5.0	6	10.8	57
7.5	4	7.2	43
10.0	3	5.4	29
15.0	2	3.6	19

3.2 Simulation results

In Fig. 5, the mean residence time of DNA molecules in the denaturation (Fig. 5a), annealing (Fig. 5b), and extension (Fig. 5c) zones is compared to the nominal residence time. The mean residence time for each zone comes from

the pertinent RTD (cf. Section S4, Fig. S4 in ESM). The temperature range for the calculation of RTDs is $[T_x - \Delta T_x, T_x + \Delta T_x]$ (x =denaturation, annealing, extension, cf. Section S5, Fig. S5a in ESM) with ΔT_x equal to 1 and 2 K. The nominal residence time is obtained from the volume of each zone over the corresponding heater divided by the volumetric flow rate (V/Q).

The mean residence time in the zones (denaturation, annealing, extension) decreases with the volumetric flow rate, resembling the decrease of the nominal residence time which is inversely proportional to the flow rate ($\propto Q^{-1}$). However, it is shown that the mean residence times for both the extension and denaturation zones are lower compared to the nominal ones, depending on the flow rate and the acceptable temperature variation (ΔT_x). In particular, for the denaturation zone, the mean residence time is ~48% of the nominal for $\Delta T_x=1$ K at 2.5 $\mu\text{l}/\text{min}$ (~86% for $\Delta T_x=2$ K) and decreases monotonically to ~33% of the nominal value for $\Delta T_x=1$ K at 20 $\mu\text{l}/\text{min}$ (~83% for $\Delta T_x=2$ K). The deviation of the mean residence time from the nominal one is higher for the extension zone, where the mean residence time is ~38% of the nominal for $\Delta T_x=1$ K at 2.5 $\mu\text{l}/\text{min}$ (~78% for $\Delta T_x=2$ K), and decreases monotonically to ~22% of the nominal value at 20 $\mu\text{l}/\text{min}$ (~44% for $\Delta T_x=2$ K). Regarding the annealing zone, the mean residence time for $\Delta T_x=1$ K is 97% of the nominal value at 2.5 $\mu\text{l}/\text{min}$ and decreases monotonically to ~67% of the nominal value at 20 $\mu\text{l}/\text{min}$. For $\Delta T_x=2$ K, good agreement (within 10%) is observed between the mean residence time and the nominal one, nearly at all flow rates. The better agreement with the nominal values in the case of annealing originates from the better temperature uniformity in the annealing zone compared to the other two zones.

The actual PCR protocols (denaturation : annealing : extension residence times) together with the nominal protocols for 2.5, 5, 7.5, 10, 15, and 20 $\mu\text{l}/\text{min}$ are shown in Table 3. Table 3 as well as Fig. 5 clearly demonstrate the effect of the temperature and velocity distributions in each zone on the PCR protocol. Indeed, the actual PCR protocol is shown to be shorter compared to the nominal one. In Table 3, it is also shown that the relative residence times (ratio of the residence time over the residence time in denaturation) of the actual protocols are disturbed (compared to the nominal one), with the relative residence time in extension approaching 1 (instead of 1.5, according to the chip geometry) at flow rates higher than 7.5 $\mu\text{l}/\text{min}$.

The actual PCR protocol for 15 $\mu\text{l}/\text{min}$, i.e. the maximum volumetric flow rate for which DNA amplification occurs (see Section 3.1.iii), is 0.7 s : 0.8 s : 0.6 s for $\Delta T_x = 2$ K (0.3 s : 0.7 s : 0.3 s for $\Delta T_x = 1$ K). The latter is proved by the experimental measurements to be the shortest effective PCR protocol. Such very short mean residence times resulting in an effective PCR protocol are justified by independent biochemical evidence concerning the PCR reaction. Indeed, the extension step, which is considered the slowest step in PCR amplification [60], is performed with an enzyme engineered to

copy DNA at a rate of 1000 bp/s [54]. According to the latter specification, ~0.2 s (for a 157 bp amplicon) is the lowest limit of the extension time for effective DNA amplification, in agreement with the actual duration of the extension step, as calculated at a flow rate of 20 $\mu\text{l}/\text{min}$ (cf. Table 3). This actual duration of the extension step was made possible at these high flow rates thanks to the intentional increase of the microchannel width (by 1.5) at the extension zone. Further decrease of the residence times in the extension or the denaturation or the annealing zones does not allow for successful DNA amplification in the microdevice reported herein, as demonstrated by gel electrophoresis.

Table 3 Actual and nominal PCR protocols for volumetric flow rates of 2.5, 5, 7.5, 10, 15, and 20 $\mu\text{l}/\text{min}$. The relative ratios of the residence times (ratios of the residence times over the residence time in denaturation) are also shown in parentheses. In all cases, one decimal digit is kept.

Volumetric flow rate ($\mu\text{l}/\text{min}$)	PCR protocols		
	denaturation : annealing : extension (in s)		
	nominal	actual, $\Delta T_x = 2 \text{ K}$	actual, $\Delta T_x = 1 \text{ K}$
2.5	4.8 : 4.8 : 7.1 (1.0 : 1.0 : 1.5)	4.2 : 5.4 : 5.6 (1.0 : 1.3 : 1.3)	2.3 : 4.7 : 2.7 (1.0 : 2.0 : 1.2)
5.0	2.4 : 2.4 : 3.6 (1.0 : 1.0 : 1.5)	2.1 : 2.6 : 2.6 (1.0 : 1.3 : 1.2)	1.0 : 2.3 : 1.2 (1.0 : 2.4 : 1.2)
7.5	1.6 : 1.6 : 2.4 (1.0 : 1.0 : 1.5)	1.4 : 1.7 : 1.6 (1.0 : 1.3 : 1.1)	0.6 : 1.5 : 0.8 (1.0 : 2.5 : 1.3)
10.0	1.2 : 1.2 : 1.8 (1.0 : 1.0 : 1.5)	1.0 : 1.3 : 1.1 (1.0 : 1.3 : 1.1)	0.5 : 1.1 : 0.5 (1.0 : 2.4 : 1.0)
15.0	0.8 : 0.8 : 1.2 (1.0 : 1.0 : 1.5)	0.7 : 0.8 : 0.6 (1.0 : 1.2 : 0.9)	0.3 : 0.7 : 0.3 (1.0 : 2.5 : 1.0)
20.0	0.6 : 0.6 : 0.9 (1.0 : 1.0 : 1.5)	0.5 : 0.6 : 0.4 (1.0 : 1.2 : 0.8)	0.2 : 0.4 : 0.2 (1.0 : 2.0 : 1.0)

4. Conclusions

In this study we present the design and fabrication of a fast, continuous-flow μPCR device with integrated resistive microheaters, manufactured in the PCB industry, all seamlessly realized, for the first time, on the same PCB substrate with PCB-compatible, industrial materials and processes (patterning and sealing). The commercially available materials for the fabrication of the proposed μPCR chip are already in use in industrial PCB manufacturing (but for different purposes), thus

facilitating the mass production of our chip using established and widely spread commercial manufacturing. The high integrability of microfluidics with other electronic components (such as sensors) offered by the PCB substrate, coupled with the potential of reliable and low cost mass production in the PCB industry, and the low power consumption of the introduced μ PCR are the main advantages of the proposed chip, thus rendering it an outstanding component for LOC diagnostic systems. Furthermore, the extremely reduced total reaction times (down to 2 min) combined with the reduced power consumption during its operation (2.7 W) suggest that this chip is also suitable for implementation in low-resource settings. Therefore, the presented device combines unique advantages never met before in a single device.

The investigation of the PCR efficiency, by calculating the residence time distribution (RTDs) of the DNA molecules within acceptable temperature limits, provides useful results regarding the actual PCR protocol that is held on the device. The temperature and velocity distributions within the PCR mixture in the device are shown to disturb the PCR protocol: Not only the actual protocol is shorter, but the ratio of the times in each zone is different compared to the nominal one. Such deviations from nominal PCR protocol design should be taken into account to result in an improved μ PCR chip design from a thermal distribution point of view. In addition, the latter may allow increase in DNA product yield for the same volumetric flow rate, or even the realization of an effective PCR protocol subjected to higher flow rates, further decreasing the total reaction time and leading to even faster diagnosis results.

Acknowledgments: This research was financially supported by: 1) FP7 “Love Wave Fully Integrated Lab-on-chip Platform for Food Pathogen Detection” – LOVE FOOD project (Contract No 317742) and 2) Horizon 2020-EU 2.1.1, Project ID: 68768, “LOVEFOOD2Market– A portable MicroNanoBioSystem and Instrument for ultra-fast analysis of pathogens in food: Innovation from LOVE-FOOD lab prototype to a pre-commercial instrument” (<http://lovefood2market.eu/>). The authors would like to thank Drs. S.E. Kakambakos and P.S. Petrou at IPRETEA, NCSR “Demokritos”, for providing access to their roll laminator.

Conflict of interest declaration

The authors declare no conflict of interest.

References

1. Arora A, Simone G, Salieb-Beugelaar GB, Kim JT, Manz A. Latest Developments in Micro Total Analysis Systems. *Anal Chem*. 2010;82(12):4830-47.
2. Trietsch SJ, Hankemeier T, van der Linden HJ. Lab-on-a-chip technologies for massive parallel data generation in the life sciences: A review. *Chemometr Intell Lab*. 2011;108(1):64-75.
3. Romao VC, Martins SAM, Germano J, Cardoso FA, Cardoso S, Freitas PP. Lab-on-Chip Devices: Gaining Ground Losing Size. *ACS Nano*. 2017;11(11):10659-64.
4. Ahmad F, Hashsham SA. Miniaturized nucleic acid amplification systems for rapid and point-of-care diagnostics: A review. *Anal Chim Acta*. 2012;733:1-15.
5. Chouler J, Di Lorenzo M. Water Quality Monitoring in Developing Countries; Can Microbial Fuel Cells be the Answer? *Biosensors*. 2015;5(3):450-70.
6. Voetsch AC, Van Gilder TJ, Angulo FJ, Farley MM, Shallow S, Marcus R, et al. FoodNet Estimate of the Burden of Illness Caused by Nontyphoidal Salmonella Infections in the United States. *Clin Infect Dis*. 2004;38(Supplement_3):S127-S34.
7. Majowicz SE, Musto J, Scallan E, Angulo FJ, Kirk M, O'Brien SJ, et al. The Global Burden of Nontyphoidal Salmonella Gastroenteritis. *Clin Infect Dis*. 2010;50(6):882-9.
8. Zhao X, Lin C-W, Wang J, Oh DH. Advances in rapid detection methods for foodborne pathogens. *J Microbiol Biotechnol*. 2014;24(3):297-312.
9. Pandey CM, Augustine S, Kumar S, Kumar S, Nara S, Srivastava S, et al. Microfluidics Based Point-of-Care Diagnostics. *Biotechnol Adv*. 2018;13(1):1700047.
10. Bruijns B, van Asten A, Tiggelaar R, Gardeniers H. Microfluidic Devices for Forensic DNA Analysis: A Review. *Biosensors*. 2016;6(3):41.
11. Khalid N, Kobayashi I, Nakajima M. Recent lab-on-chip developments for novel drug discovery. *Wiley Interdiscip Rev Syst Biol Med*. 2017;9(4):e1381.
12. Mullis K, Faloona F, Scharf S, Saiki R, Horn G, Erlich H, editors. Specific enzymatic amplification of DNA in vitro: the polymerase chain reaction. Cold Spring Harbor symposia on quantitative biology 1986: Cold Spring Harbor Laboratory Press
13. Roper MG, Easley CJ, Landers JP. Advances in Polymerase Chain Reaction on Microfluidic Chips. *Anal Chem*. 2005;77(12):3887-94.
14. Zhang C, Xu J, Ma W, Zheng W. PCR microfluidic devices for DNA amplification. *Biotechnol Adv*. 2006;24(3):243-84.
15. Zhang C, Xing D. Miniaturized PCR chips for nucleic acid amplification and analysis: latest advances and future trends. *Nucleic Acids Res*. 2007;35(13):4223-37.
16. Park S, Zhang Y, Lin S, Wang T-H, Yang S. Advances in microfluidic PCR for point-of-care infectious disease diagnostics. *Biotechnol Adv*. 2011;29(6):830-9.
17. Zhang Y, Ozdemir P. Microfluidic DNA amplification—A review. *Anal Chim Acta*. 2009;638(2):115-25.
18. Northrup MA, Gonzalez C, Hadley D, Hills RF, Landre P, Lehew S, et al., editors. A Mems-based Miniature DNA Analysis System. *Transducers '95 1995 25-29 June 1995*.
19. Xiang Q, Xu B, Fu R, Li D. Real Time PCR on Disposable PDMS Chip with a Miniaturized Thermal Cycler. *Biomed Microdevices*. 2005;7(4):273-9.
20. Kopp MU, De Mello AJ, Manz A. Chemical amplification: Continuous-flow PCR on a chip. *Science*. 1998;280(5366):1046-8.
21. Wang H, Chen J, Zhu L, Shadpour H, Hupert ML, Soper SA. Continuous Flow Thermal Cycler Microchip for DNA Cycle Sequencing. *Anal Chem*. 2006;78(17):6223-31.
22. Moschou D, Vourdas N, Kokkoris G, Papadakis G, Parthenios J, Chatzandroulis S, et al. All-plastic, low-power, disposable, continuous-flow PCR chip with integrated microheaters for rapid DNA amplification. *Sens Actuators B Chem*. 2014;199:470-8.
23. Sun Y, Kwok Y-C, Foo-Peng Lee P, Nguyen N-T. Rapid amplification of genetically modified organisms using a circular ferrofluid-driven PCR microchip. *Anal Bioanal Chem*. 2009;394(5):1505-8.
24. Tsung-Min H, Ching-Hsing L, Gwo-Bin L, Chia-Sheng L, Fu-Chun H. A Micromachined Low-power-consumption Portable PCR System. *J Med Biol Eng*. 2006;26(1):43-9.
25. Papadopoulos VE, Kokkoris G, Kefala IN, Tserepi A. Comparison of continuous-flow and static-chamber μ PCR devices through a computational study: the potential of flexible polymeric substrates. *Microfluid Nanofluidics*. 2015;19(4):867-82.
26. Volpatti LR, Yetisen AK. Commercialization of microfluidic devices. *Trends Biotechnol*. 2014;32(7):347-50.
27. Mohammed MI, Haswell S, Gibson I. Lab-on-a-chip or Chip-in-a-lab: Challenges of Commercialization Lost in Translation. *Proc Technol*. 2015;20(Supplement C):54-9.

28. Duchesne L, Lacombe K. Innovative technologies for point-of-care testing of viral hepatitis in low-resource and decentralized settings. *J Viral Hepat.* 2018;25(2):108-17.
29. Walsh DI, Kong DS, Murthy SK, Carr PA. Enabling Microfluidics: from Clean Rooms to Makerspaces. *Trends Biotechnol.* 2017;35(5):383-92.
30. Merkel T, Graeber M, Pagel L. New technology for fluidic microsystems based on PCB technology. *Sens Actuators A Phys.* 1999;77(2):98-105.
31. Gaßmann S, Ibendorf I, Pagel L. Realization of a flow injection analysis in PCB technology. *Sens Actuators A Phys.* 2007;133(1):231-5.
32. Aracil C, Perdignes F, Moreno JM, Luque A, Quero JM. Portable Lab-on-PCB platform for autonomous micromixing. *Microelectron Eng.* 2015;131:13-8.
33. Moschou D, Tserepi A. The lab-on-PCB approach: tackling the μ TAS commercial upscaling bottleneck. *Lab Chip.* 2017;17(8):1388-405.
34. Nguyen N-T, Huang X. Miniature valveless pumps based on printed circuit board technique. *Sens Actuators A Phys.* 2001;88(2):104-11.
35. Ingle AP, Duran N, Rai M. Bioactivity, mechanism of action, and cytotoxicity of copper-based nanoparticles: A review. *Appl Microbiol Biot.* 2014;98(3):1001-9.
36. Li J, Wang Y, Dong E, Chen H. USB-driven microfluidic chips on printed circuit boards. *Lab Chip.* 2014;14(5):860-4.
37. Metz S, Holzer R, Renaud P. Polyimide-based microfluidic devices. *Lab Chip.* 2001;1(1):29-34.
38. Mavraki E, Moschou D, Kokkoris G, Vourdas N, Chatzandroulis S, Tserepi A. A continuous flow μ PCR device with integrated microheaters on a flexible polyimide substrate. *Procedia Eng.* 2011;25:1245-8.
39. Wangler N, Gutzweiler L, Kalkandjiev K, Müller C, Mayenfels F, Reinecke H, et al. High-resolution permanent photoresist laminate TMMF for sealed microfluidic structures in biological applications. *J Micromech Microeng.* 2011;21(9):095009.
40. Wu LL, Marshall LA, Babikian S, Han CM, Santiago JG, Bachman M, editors. A printed circuit board based microfluidic system for point-of-care diagnostics applications. 15th International Conference on Miniaturized Systems for Chemistry and Life Sciences (MicroTAS) 2011.
41. Wu LL, Babikian S, Li GP, Bachman M, editors. Microfluidic printed circuit boards. Proceedings - Electronic Components and Technology Conference 2011.
42. Vasilakis N, Moschou D, Carta D, Morgan H, Prodromakis T. Long-lasting FR-4 surface hydrophilisation towards commercial PCB passive microfluidics. *Appl Surf Sci.* 2016;368:69-75.
43. Papadopoulos VE, Kefala IN, Kaprou G, Kokkoris G, Moschou D, Papadakis G, et al. A passive micromixer for enzymatic digestion of DNA. *Microelectron Eng.* 2014;124:42-6.
44. Kefala IN, Papadopoulos VE, Karpou G, Kokkoris G, Papadakis G, Tserepi A. A labyrinth split and merge micromixer for bioanalytical applications. *Microfluid Nanofluidics.* 2015;19(5):1047-59.
45. Kaprou G, Papadakis G, Papageorgiou D, Kokkoris G, Papadopoulos V, Kefala I, et al. Miniaturized devices for isothermal DNA amplification addressing DNA diagnostics. *Microsyst Technol.* 2016;22(7):1529-34.
46. Temiz Y, Lovchik RD, Kaigala GV, Delamarche E. Lab-on-a-chip devices: How to close and plug the lab? *Microelectron Eng.* 2015;132:156-75.
47. Becker H, Gärtner C. Polymer microfabrication technologies for microfluidic systems. *Anal Bioanal Chem.* 2008;390(1):89-111.
48. Kaprou G, Papadakis G, Kokkoris G, Papadopoulos V, Kefala I, Papageorgiou D, et al., editors. Miniaturized devices towards an integrated lab-on-a-chip platform for DNA diagnostics. *Progress in Biomedical Optics and Imaging - Proceedings of SPIE*; 2015.
49. Cao Q, Kim M-C, Klapperich C. Plastic microfluidic chip for continuous-flow polymerase chain reaction: Simulations and experiments. *Biotechnol Adv.* 2011;6(2):177-84.
50. Ltd E. Technical Terms and Abbreviations. Available from: <https://www.eurocircuits.com/technical-terms-and-abbreviations/>.
51. Tserepi A., Chatzandroulis S., Kaprou G., Kokkoris G., Ellinas K., Papageorgiou D., inventor Microfluidic reactors and process for their production. Greece patent GRA 20170100305
- 2017 30.06.2017.
52. Tserepi A., Chatzandroulis S., Kaprou G., Kokkoris G., Ellinas K., Papageorgiou D., inventor Microfluidic reactors and process for their production patent 18386020.4-1101. 2018 29.06.18.
53. Vorkas PA, Christopoulos K, Kroupis C, Lianidou ES. Mutation scanning of exon 20 of the BRCA1 gene by high-resolution melting curve analysis. *Clin Biochem.* 2010;43(1-2):178-85.
54. KAPABIOSYSTEMS. <https://www.kapabiosystems.com/product-applications/products/pcr-2/kapa2g-fast-pcr-kits/>.
55. Leonard WF, Yu HY. Thermoelectric power of thin copper films. *J Appl Phys.* 1973;44(12):5320-3.
56. Kim YS. Microheater-integrated single gas sensor array chip fabricated on flexible polyimide substrate. *Sens Actuators B Chem.* 2006;114(1):410-7.

57. Shen K, Chen X, Guo M, Cheng J. A microchip-based PCR device using flexible printed circuit technology. *Sens Actuators B Chem.* 2005;105(2):251-8.
58. Wheeler EK, Benett W, Stratton P, Richards J, Chen A, Christian A, et al. Convectively Driven Polymerase Chain Reaction Thermal Cyclers. *Anal Chem.* 2004;76(14):4011-6.
59. Jiang L, Mancuso M, Lu Z, Akar G, Cesarman E, Erickson D. Solar thermal polymerase chain reaction for smartphone-assisted molecular diagnostics. *Sci Rep.* 2014;4:4137.
60. Hashimoto M, Chen P-C, Mitchell MW, Nikitopoulos DE, Soper SA, Murphy MC. Rapid PCR in a continuous flow device. *Lab Chip.* 2004;4(6):638-45.

Author accepted manuscript

Figure Captions

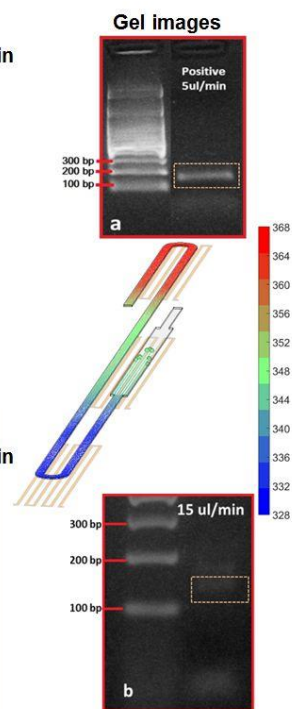
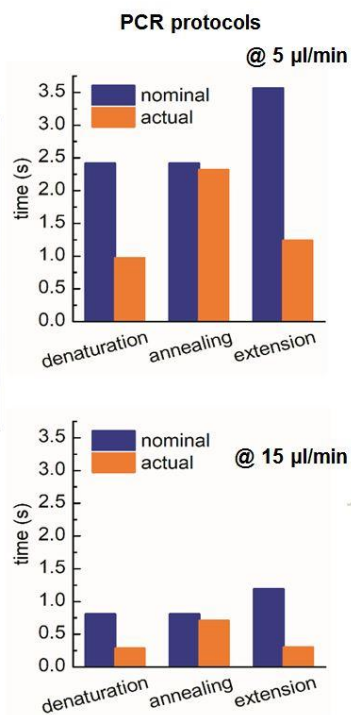
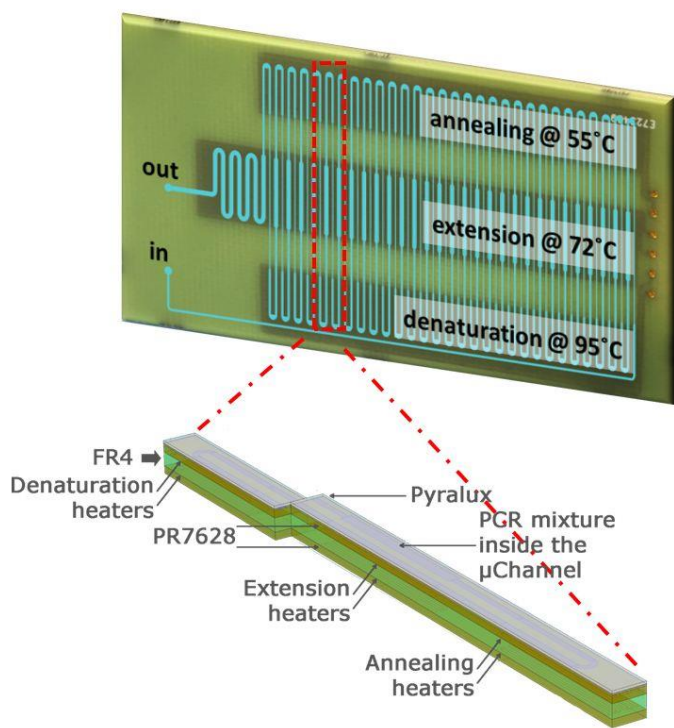
Fig. 1 a) Image of 3 PCB-embedded Cu microheaters, custom-designed and fabricated at PCB vendor b) Image of a continuous flow μ PCR device (non-sealed for clearly viewing the microchannel), employing 30 cycles, fabricated on a PCB substrate with embedded microheaters

Fig. 2 Schematic of the unit cell where the calculations take place

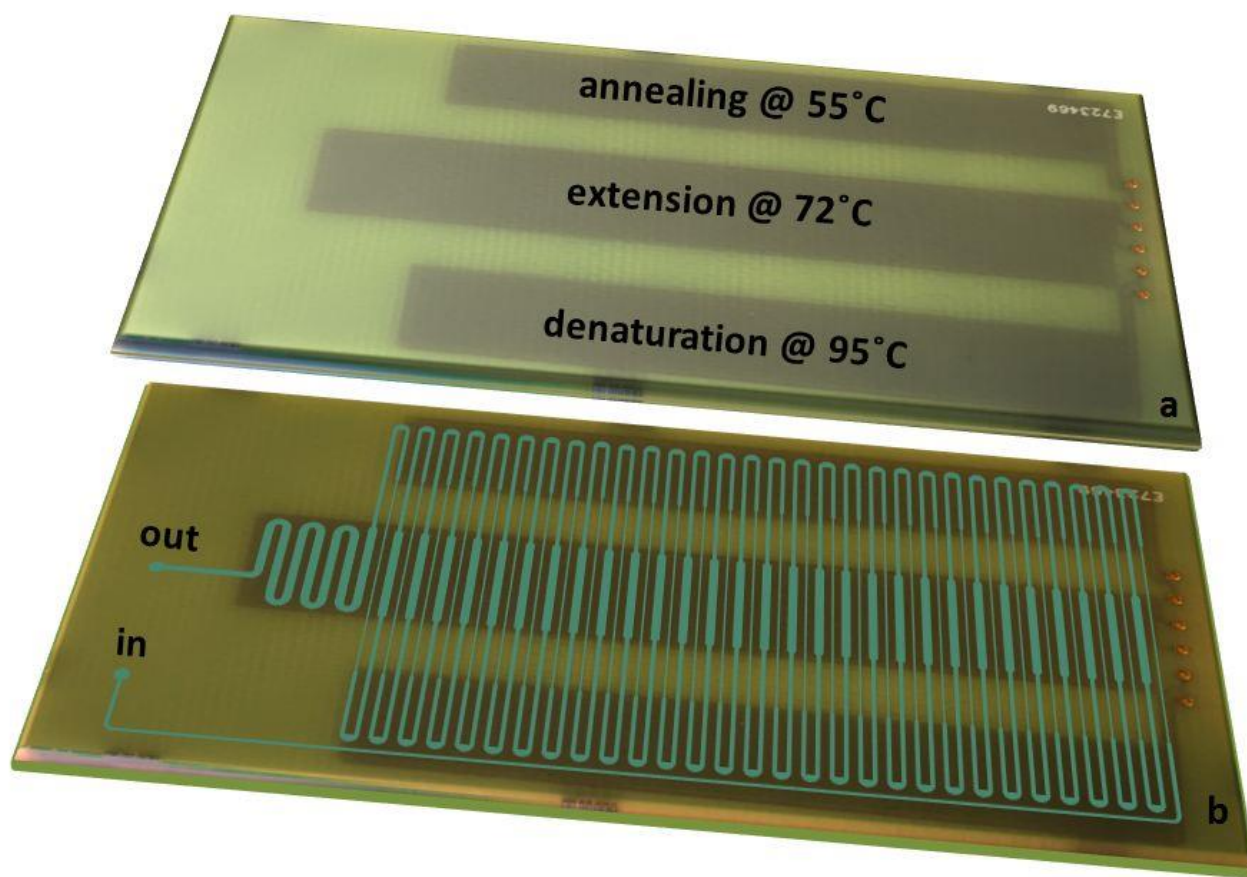
Fig. 3 Images of agarose gels depicting DNA ladder (on the left of each image) and 157 bp DNA amplicons (on the right of each image) from the μ PCR device (a, b), operating at different flow rates a) 5 μ l/min, b) 7.5 μ l/min and 10 μ l/min, and c) conventional thermocycler with 10 sec residence time at each temperature

Fig. 4 Images of agarose gels depicting a) 198 bp DNA amplicons (on the left) from the μ PCR device, operating at a flow rate of 7.5 μ l/min, and the DNA ladder (on the right), b) 395 bp amplicons (on the right) from the μ PCR device, operating at a flow rate of 7.5 μ l/min, and the DNA ladder (on the left)

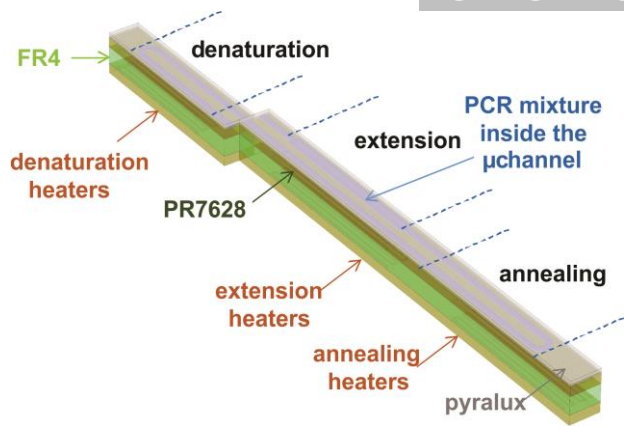
Fig. 5 Mean residence time at the (a) denaturation, (b) annealing, and (c) extension temperatures when ΔT_x equals 1 and 2 K, compared to the nominal residence time



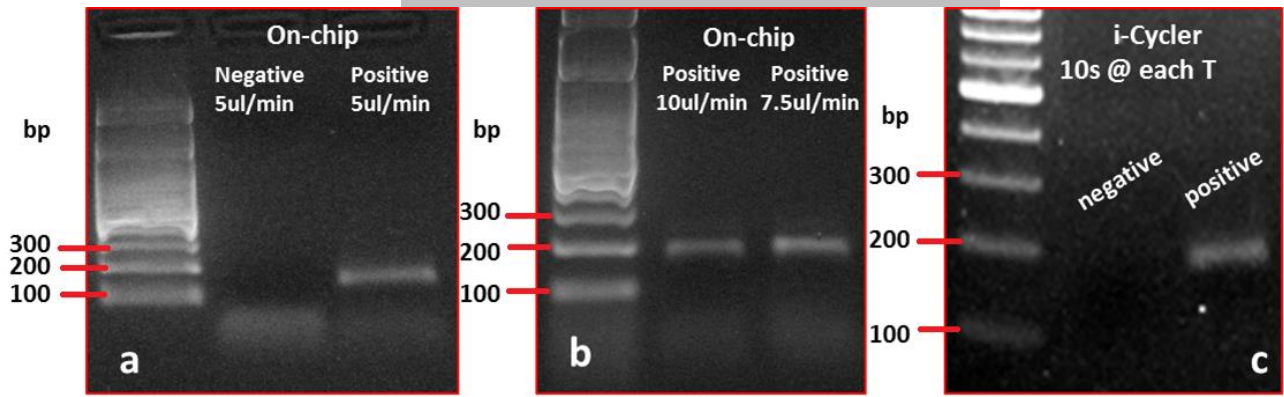
Author accepted m



Author accep



Author accepted manuscript



Author accepted manuscript

